



Accepted Article

Title: B33– and B34–: Aromatic Planar Boron Clusters with A Hexagonal Vacancy

Authors: Qiang Chen, Wei-Li Li, Xiao-Yun Zhao, Hai-Ru Li, Lin-Yan Feng, Hua-Jin Zhai, Si-Dian Li, and Lai-Sheng Wang

This manuscript has been accepted after peer review and appears as an Accepted Article online prior to editing, proofing, and formal publication of the final Version of Record (VoR). This work is currently citable by using the Digital Object Identifier (DOI) given below. The VoR will be published online in Early View as soon as possible and may be different to this Accepted Article as a result of editing. Readers should obtain the VoR from the journal website shown below when it is published to ensure accuracy of information. The authors are responsible for the content of this Accepted Article.

To be cited as: *Eur. J. Inorg. Chem.* 10.1002/ejic.201700573

Link to VoR: <http://dx.doi.org/10.1002/ejic.201700573>

B₃₃ and B₃₄ : Aromatic Planar Boron Clusters with A Hexagonal Vacancy

Qiang Chen,^[a,c] Wei-Li Li,^[b] Xiao-Yun Zhao,^[a] Hai-Ru Li,^[a] Lin-Yan Feng,^[a] Hua-Jin Zhai,^{*,[a]} Si-Dian Li,^{*,[a]} and Lai-Sheng Wang^{*,[b]}

Abstract: Systematic experimental and theoretical studies have shown that anionic boron clusters (B_n⁻) possess planar or quasi-planar (2D) structures in a wide range of cluster size. The 2D structures consist of B₃ triangles often decorated with tetragonal and pentagonal defects. As *n* increases, hexagonal vacancies appear to be a key structural feature, which underlies the stability of borophenes. The correlation of the defects with cluster size is important to understand the stability and structural evolution of boron clusters. Here we report an investigation of the structures and chemical bonding of B₃₃ and B₃₄ using photoelectron spectroscopy (PES) and density-functional theory (DFT) calculations. Global minimum searches reveal that the potential landscapes of B₃₃ and B₃₄ are dominated by 2D isomers. Comparisons between experiment and theory confirm that their global-minimum structures are both 2D with a hexagonal vacancy (C_s B₃₃) and (C₁ B₃₄), with the latter being a chiral cluster. Bonding analyses indicate that the C_s B₃₃ cluster possesses ten delocalized bonds, analogous to those in the polycyclic aromatic hydrocarbon C₁₉H₁₁. Bonding analyses on the equivalent closed-shell B₃₄²⁻ species show that its 12 delocalized bonds consist of two separate aromatic systems: nine exterior and three interior bonds.

Introduction

Boron clusters are interesting because of the prospects to discover boron analogues of the celebrated carbon fullerenes, graphene, and nanotubes.^[1-3] Early theoretical studies suggested that the B₁₂ icosahedral unit prevalent in bulk boron^[4] is not stable as isolated clusters relative to planar or quasi-planar (2D) structures.^[5-13] Over the past decade, joint experimental and theoretical investigations have uncovered a rich 2D world for size-selected boron clusters.^[14-42] Ion mobility measurements in combination with density-functional theory

(DFT) calculations suggested that cationic B_n⁺ clusters have 2D structures up to *n* = 16.^[14] Theoretical calculations showed that the critical size of 2D to 3D tubular transition for neutral boron clusters occurs at B₂₀,^[30] even though the tubular structure was not observed in an infrared spectroscopy study.^[17,43] The most extensive experimental studies have been on size-selected negatively-charged boron clusters (B_n⁻) using photoelectron spectroscopy (PES).^[17] Joint PES and theoretical investigations have shown 2D structures exist up to *n* = 40.^[15-42] Chemical bonding analyses revealed that 2D boron clusters are characterized by both delocalized and d bonding, resulting in concepts of aromaticity, antiaromaticity, and all-boron analogues of hydrocarbons.^[15-44]

The 2D B_n clusters elucidated by joint PES and theoretical studies are all composed of B₃ triangles often with tetragonal, pentagonal, and hexagonal vacancies as the cluster size increases. These polygonal defects or vacancies play critical roles in the stability of the 2D boron clusters.^[26-42] Interestingly, the presence of these defects results in structural fluxionality in the cluster plane,^[16,17,29] which have inspired proposals of molecular Wankel motors and other dynamic effects.^[45-51] The first 2D boron cluster discovered to contain a hexagonal vacancy was B₃₆, which was observed to have pseudo-C_{6v} symmetry.^[41] Neutral B₃₆ has perfect C_{6v} symmetry and can serve as a basic building unit for 2D boron monolayers, for which a name borophene was proposed.^[41] The hexagonal B₃₆ cluster provided the first indirect experimental evidence for the viability of borophenes. The double-hexagonal vacancy observed in B₃₅ makes it an even more flexible motif to construct borophenes.^[40] The global minimum of B₃₀ was found to be a 2D chiral structure with a hexagonal vacancy.^[39] The smallest boron cluster (B₂₆) with a hexagonal vacancy was reported recently,^[35] whereas B₃₇ and B₃₈ was found very recently to contain a double-hexagonal vacancy similar to that in B₃₅.^[42] Another major breakthrough in size-selected boron clusters is the discovery of the first all-boron fullerenes, D_{2d} B₄₀⁰, named borospherenes using joint PES and theoretical studies.^[52] Even though the global minimum of B₄₀ is a 2D structure with the B₄₀ borospherene as a co-existing isomer, the neutral B₄₀ borospherene is the overwhelming global minimum. Subsequently, B₃₉ was found to consist of two close-lying chiral borospherenes of C₃ and C₂ symmetries.^[53] Less symmetric and seashell-like B₂₈ and B₂₉ borospherenes were also observed experimentally as low-lying isomers.^[37,38]

The size of the vacancy seems to increase with cluster size in 2D boron clusters from tetragonal to pentagonal and hexagonal. The first double-hexagonal vacancy appeared in B₃₅.^[40] Hence, the clusters from B₃₁ to B₃₄ represent the size range where the cluster structure evolves from a single hexagonal vacancy to a double-hexagonal vacancy. However, these four critical clusters have not been studied heretofore. In the present work, we report an investigation on the structures and chemical bonding of B₃₃ and B₃₄ using PES in conjunction

[a] Q. Chen, X. Y. Zhao, H. R. Li, L. Y. Feng, H. J. Zhai, S. D. Li
Nanocluster Laboratory
Institute of Molecular Science
Shanxi University
Taiyuan 030006 (China)
E-mail: hj.zhai@sxu.edu.cn, lisidian@sxu.edu.cn

[b] W. L. Li, L. S. Wang
Department of Chemistry
Brown University
Providence, RI 02912 (USA)
E-mail: Lai-Sheng_Wang@brown.edu
URL: casey.brown.edu/chemistry/research/LSWang/

[c] Q. Chen
Beijing National Laboratory for Molecular Sciences
State Key Laboratory for Structural Chemistry of Unstable and Stable Species, Institute of Chemistry, Chinese Academy of Sciences, Beijing 100190 (China)

with global minimum searches and DFT calculations. The global minima of both B_{33} and B_{34} are identified as 2D structures with a single hexagonal vacancy, with B_{34} being chiral similar to the chiral B_{30} .^[39]

Results

Photoelectron Spectroscopy

The PES experiment was done with a magnetic bottle electron analyzer equipped with a laser-vaporization cluster source.^[17,54] The PE spectra of B_{33} and B_{34} are shown in Figures 1 and 2, respectively, in comparison with simulated spectra from the respective global minimum. The observed spectral features are labeled with letters (X, A, δ , E) and the measured vertical detachment energies (VDEs) are given in Table S1.

The PE spectrum of B_{33} shown in Figure 1a is fairly congested. Six spectral bands (X, A, δ , E) can be identified, though each may contain multiple detachment channels. The adiabatic detachment energy (ADE) for the ground state band X (VDE: 4.09 eV) was evaluated from its leading edge as 3.91 ± 0.06 eV, which also represents the electron affinity (EA) of neutral B_{33} . Band A is weaker with a VDE of 4.62 eV, beyond which the spectrum is nearly continuous. The labels from B to E are for the sake of discussion only.

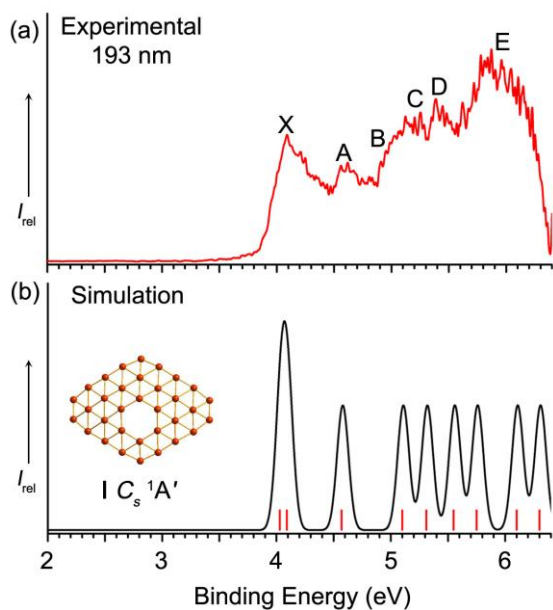


Figure 1. The photoelectron spectrum of (a) B_{33} at 193 nm (6.424 eV), compared to (b) the simulated spectrum of the global minimum of B_{33} (I, C_s). Vertical bars in (b) denote calculated VDEs at the TD-PBE0/6-311+G(d) level.

The PE spectrum of B_{34} (Figure 2a) displays two separated spectral regions. In the lower binding energy region, three overlapping bands (X, A, B) are observed between 3.5 and 4.5 eV with VDEs of 3.89, 4.02, and 4.28 eV respectively. The ADE of band X, that is, the EA of neutral B_{34} , is estimated to be 3.75 ± 0.06 eV from the band onset. In the higher binding energy region beyond 4.7 eV, the spectrum is even more congested with higher relative intensities. Three bands (C, D, E) can be tentatively identified, each being expected to contain multiple detachment transitions.

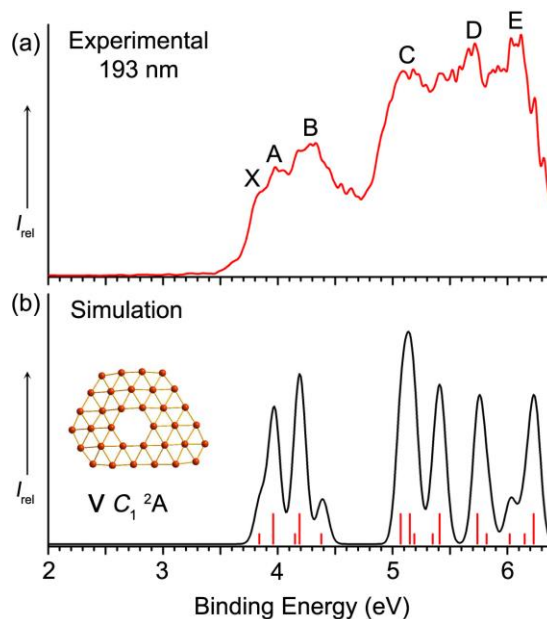


Figure 2. The photoelectron spectrum of (a) B_{34} at 193 nm, compared to (b) the simulated spectrum of the global minimum of B_{34} . Vertical bars in (b) denote calculated VDEs at the TD-PBE0/6-311+G(d) level. The longer bars are for triplet final states and the shorter ones for singlet final states.

Computational Results

The global minima of B_{33} and B_{34} were searched using the TGMIn code.^[55,56] Candidate structures were subsequently reoptimized at the PBE0/6-311+G(d) level.^[57-59] Low-lying isomers of B_{33} and B_{34} within 1 eV are shown in Figures S1 and S2, respectively. The four lowest-lying structures of B_{33} and B_{34} are presented in Figure 3. All the relative energies were corrected for zero-point energies (ZPEs). Cartesian coordinates for the most stable B_{33} and B_{34} clusters are given in Table S2.

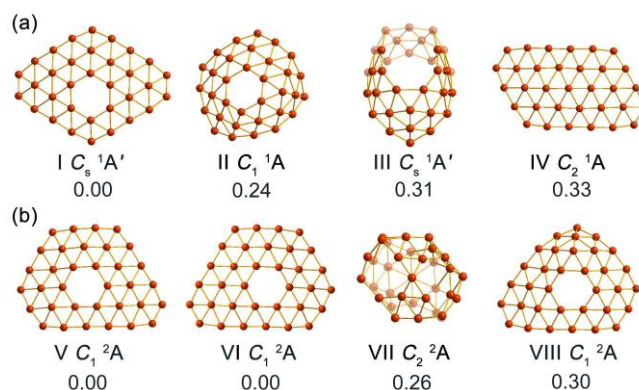


Figure 3. The global minimum and low-lying isomers of (a) B_{33} and (b) B_{34} . Relative energies at the PBE0/6-311+G(d) level (including ZPE corrections) are shown in eV. Note the global minimum of B_{34} (V and VI) are enantiomers.

Global minimum and low-lying isomers of B_{33}

The global minimum of B_{33} is 2D (I C_s , $^1A'$) with an overall diamond shape and a central hexagonal vacancy (Figure 3a). The 2D structure, consisting of eighteen peripheral and fifteen interior atoms, is quasi-planar with an out-of-plane distortion of 1.72 Å. At the PBE0/6-311+G(d) levels, isomers II, III, and IV are 0.24, 0.31, and 0.33 eV above the global minimum, respectively. Isomer II (C_1 , 1A) is a severely distorted 2D structure with a hexagonal vacancy and a filled pentagon. Isomer III (C_s , $^1A'$) is a

the bonding analyses.^[61] We also analyzed the bonding for the closed-shell B_{34} (see Figure S6).

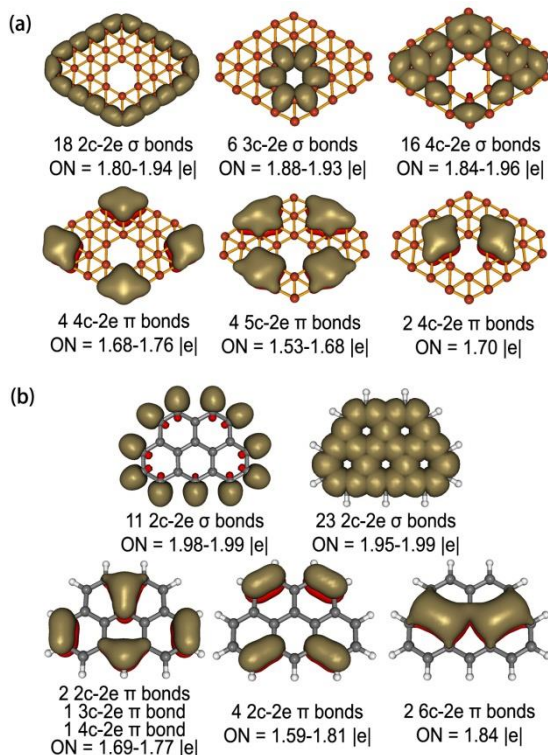


Figure 4. Results of the AdNDP analyses for (a) $C_{2v} B_{33}$ and (b) $C_{2v} C_{19}H_{11}$.

Among the 100 valence electrons in B_{33} , the AdNDP analysis recovered eighteen localized peripheral 2c-2e σ B bonds, six 3c-2e bonds around the central hexagon, and sixteen 4c-2e bonds between the inner hexagon and the cluster periphery (Figure 4a). The remaining valence electrons form ten delocalized π bonds. Interestingly, the bonding in the 2D B_{33} is similar to that in the polycyclic aromatic hydrocarbon $C_{19}H_{11}$ (Figure 4b), suggesting the aromatic character of the boron cluster. Thus, the 2D B_{33} cluster can be considered as a new example of all-boron analogues of hydrocarbons.^[17,23-29,32,39-42]

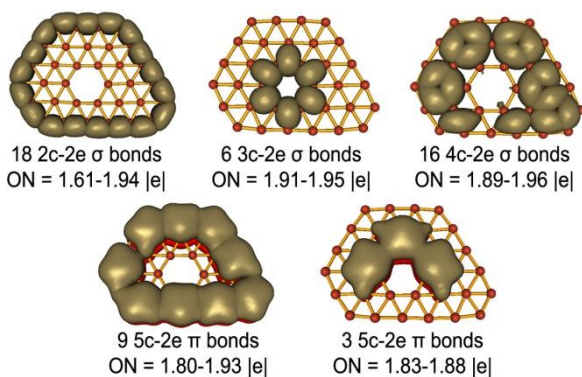


Figure 5. Results of the AdNDP analysis for the closed-shell $C_s B_{34}$.

The B_{34}^{2-} (Figure 5) is almost identical to that in B_{33} . Among the 104 valence electrons, there are eighteen peripheral 2c-2e σ B bonds, six 3c-2e bonds around the central hexagon, and sixteen 4c-2e bonds between the inner hexagon and the cluster periphery. However, the π bonding in the 2D B_{34}^{2-} species is slightly different and can be seen to consist of two delocalized π systems, including nine 5c- σ π

bonds around the periphery and three 5c- σ π bonds around the inner hexagon. Each system obeys the $4N+2$ Hückel rule for aromaticity. This observation suggests that the 2D B_{34}^{2-} cluster can be considered to be doubly π -aromatic. The bonding in the 2D neutral B_{34} (Figure S6) is identical to that in the 2D B_{34}^{2-} , except that there are only two 5c- σ π bonds around the inner hexagon, making this system antiaromatic. The latter may underlie the reason why the 2D B_{34} neutral is less stable than the 3D isomer (Figure S3).

Structural Evolution in Mid-Sized Boron Clusters

It should be noted that the hexagonal vacancy, essential for the stability of borophenes,^[41] is the most important structural feature in mid-sized boron clusters, starting from B_{26} .^[35] The role of the hexagonal vacancy in the stability of B_{36} has been further analyzed recently.^[62] The hexagonal vacancy in the global minima of B_{33} and B_{34} implies that B_{35} is the smallest cluster to possess a double-hexagonal vacancy.^[40] It is interesting to see the evolution of the double-hexagonal vacancy among the low-lying isomers in B_{33} and B_{34} . In B_{33} (Figure S1), the first isomer with a double-hexagonal vacancy is 0.9 eV above the global minimum, whereas in B_{34} (Figure S2) the first isomer with a double-hexagonal vacancy is only 0.42 eV above the global minimum. The isomer with a double-hexagonal vacancy seems to gain stability from B_{33} to B_{35} , where it becomes the global minimum. It should be noted that among the low-lying isomers of B_{34} there appears an isomer with a triple-hexagonal vacancy being 0.87 eV above the global minimum. Such structural features are reminiscent of those in the V_8 borophene,^[63] consisting of roles of hexagonal vacancies.

Conclusions

We have studied the structures and chemical bonding of the B_{33} and B_{34} clusters using photoelectron spectroscopy and DFT calculations. Global minimum searches in conjunction with the experiment show that the most stable structures of both B_{33} and B_{34} are 2D with a central hexagonal vacancy. The global minimum of B_{33} has C_s symmetry, whereas that of B_{34} is chiral with C_1 symmetry. Chemical bonding analyses reveal that the 2D B_{33} and B_{34} are aromatic with the π bonding in B_{33} being analogous to that in the $C_{19}H_{11}$ polycyclic aromatic hydrocarbon. The current study confirms that the B_{35} cluster is the smallest boron cluster to feature a double-hexagonal vacancy.

Methods Section

Photoelectron spectroscopy: The experiments were carried out using a magnetic-bottle PES apparatus equipped with a laser vaporization supersonic cluster source, details of which can be found elsewhere.^[17,54] Boron clusters were produced by laser vaporization of a hot-pressed ^{10}B -enriched disk target. Clusters formed in the nozzle were entrained by a He carrier gas seeded with 5% Ar and underwent a supersonic expansion. Negatively-charged clusters were extracted from the collimated cluster beam after a skimmer and analyzed using time-of-flight mass spectrometry. The B_{33} and B_{34} clusters of interest were mass-selected and decelerated before being intercepted by a detachment laser beam. Owing to the relatively high binding energies of B_{33} and B_{34} , the 193 nm (6.424 eV) radiation from an ArF excimer laser was used to

conduct the experiment. Photoelectrons were collected at nearly 100% efficiency using a magnetic bottle and analyzed in a 3.5 m long electron flight tube. The PE spectra were calibrated using the known spectrum of Au. The energy resolution of the instrument was $8E_k/E_k \approx 2.5\%$, that is, ~ 25 meV for 1 eV kinetic energy electrons.

Computational methods: We conducted global minimum searches for B_{33} and B_{34} using an improved Basin-Hopping (BH) algorithm implemented in the TGMIn code,^[55,56] which has proved to be effective for B_n ($n = 30, 35, 38$) clusters.^[39-42] Structural searches for the closed-shell B_{33} were straightforward, but for the open-shell B_{34} we first did the structural search using the closed-shell B_{34}^2 species to save computational time. Subsequently, low-lying isomers of B_{34}^2 were detached by one electron to achieve the B_{34} isomers with further structural optimization. For each anion cluster, four different 2D structures and one random 3D isomer were used as seed structures to run the BH searches. A total of 2760 and 2721 stationary points were probed for B_{33} and B_{34}^2 , respectively. In addition, manual structural constructions were also used to aid the searches for the typical 3D double/triple-ring tubular structures and facile 2D structures based on 2D B_n ($n = 26, 30, 35, 38$) clusters.^[35-42]

The obtained low-lying isomers of B_{33} and B_{34} were re-optimized at the PBE0/6-311+G(d) level.^[57-59] Vibrational frequencies were calculated at the same level to ensure that the reported structures are true minima on the potential energy surfaces. For comparison with experimental data, VDEs and ADEs were computed for low-lying isomers of B_{33} and B_{34} at the TD-PBE0/6-311+G(d) level.^[60] PBE0 and TD-PBE0 calculations were done using the Gaussian 09 package.^[64] Bonding analyses were performed using the AdNDP method^[61] and visualized via Molekel 5.4.0.8.^[65]

Acknowledgements

The experimental work done at Brown University was supported by the US National Science Foundation (CHE-1263745). The theoretical work was supported by the National Natural Science Foundation of China (21373130 and 21573138). H.J.Z. gratefully acknowledges the support of the Sanjin Scholar distinguished professors program.

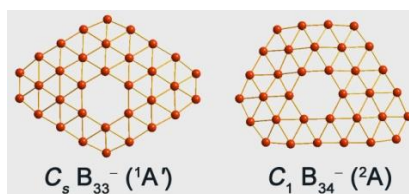
Keywords: borophenes

- [1] H. W. Kroto, J. R. Heath, S. C. O'Brien, R. F. Curl, R. E. Smalley, *Nature* **1985**, *318*, 162-163.
- [2] S. Iijima, *Nature* **1991**, *354*, 56-58.
- [3] K. S. Novoselov, A. K. Geim, S. V. Morozov, D. Jiang, Y. Zhang, S. V. Dubonos, I. V. Grigorieva, A. A. Firsov, *Science* **2004**, *306*, 666-669.
- [4] B. Albert, H. Hillebrecht, *Angew. Chem. Int. Ed.* **2009**, *48*, 8640-8668; *Angew. Chem.* **2009**, *121*, 8794-8824.
- [5] R. Kawai, J. H. Weare, *J. Chem. Phys.* **1991**, *95*, 1151-1159.
- [6] V. Bonacic-Koutecky, P. Fantucci, J. Koutecky, *Chem. Rev.* **1991**, *91*, 1035-1108.
- [7] R. Kawai, J. H. Weare, *Chem. Phys. Lett.* **1992**, *191*, 311-314.
- [8] I. Boustani, *Int. J. Quantum Chem.* **1994**, *52*, 1081-1111.
- [9] H. Kato, K. Yamashita, K. Morokuma, *Chem. Phys. Lett.* **1992**, *190*, 361-366.
- [10] A. Ricca, C. W. Bauschlicher, Jr., *Chem. Phys.* **1996**, *208*, 233-242.
- [11] I. Boustani, *Phys. Rev. B* **1997**, *55*, 16426-16438.
- [12] F. L. Gu, X. Yang, A. Tang, H. Jiao, P. v. R. Schleyer, *J. Comput. Chem.* **1998**, *19*, 203-214.
- [13] J. E. Fowler, J. M. Ugalde, *J. Phys. Chem. A* **2000**, *104*, 397-403.

- [14] E. Oger, N. R. M. Crawford, R. Kelting, P. Weis, M. M. Kappes, R. Ahlrichs, *Angew. Chem. Int. Ed.* **2007**, *46*, 8503-8506; *Angew. Chem.* **2007**, *119*, 8656-8659.
- [15] A. N. Alexandrova, A. I. Boldyrev, H. J. Zhai, L. S. Wang, *Coord. Chem. Rev.* **2006**, *250*, 2811-2866.
- [16] A. P. Sergeeva, I. A. Popov, Z. A. Piazza, W. L. Li, C. Romanescu, L. S. Wang, A. I. Boldyrev, *Acc. Chem. Res.* **2014**, *47*, 1349-1358.
- [17] L. S. Wang, *Int. Rev. Phys. Chem.* **2016**, *35*, 69-142.
- [18] H. J. Zhai, L. S. Wang, A. N. Alexandrova, A. I. Boldyrev, V. G. Zakrzewski, *J. Phys. Chem. A* **2003**, *107*, 9319-9328.
- [19] H. J. Zhai, L. S. Wang, A. N. Alexandrova, A. I. Boldyrev, *J. Chem. Phys.* **2002**, *117*, 7917-7924.
- [20] A. N. Alexandrova, A. I. Boldyrev, H. J. Zhai, L. S. Wang, E. Steiner, P. W. Fowler, *J. Phys. Chem. A* **2003**, *107*, 1359-1369.
- [21] A. N. Alexandrova, A. I. Boldyrev, H. J. Zhai, L. S. Wang, *J. Chem. Phys.* **2005**, *122*, 054313.
- [22] A. N. Alexandrova, A. I. Boldyrev, H. J. Zhai, L. S. Wang, *J. Phys. Chem. A* **2004**, *108*, 3509-3517.
- [23] H. J. Zhai, A. N. Alexandrova, K. A. Birch, A. I. Boldyrev, L. S. Wang, *Angew. Chem. Int. Ed.* **2003**, *42*, 6004-6008; *Angew. Chem.* **2003**, *115*, 6186-6190.
- [24] A. N. Alexandrova, H. J. Zhai, L. S. Wang, A. I. Boldyrev, *Inorg. Chem.* **2004**, *43*, 3552-3554.
- [25] L. L. Pan, J. Li, L. S. Wang, *J. Chem. Phys.* **2008**, *129*, 024302.
- [26] H. J. Zhai, B. Kiran, J. Li, L. S. Wang, *Nat. Mater.* **2003**, *2*, 827-833.
- [27] A. P. Sergeeva, D. Y. Zubarev, H. J. Zhai, A. I. Boldyrev, L. S. Wang, *J. Am. Chem. Soc.* **2008**, *130*, 7244-7246.
- [28] A. P. Sergeeva, B. B. Averkiev, H. J. Zhai, A. I. Boldyrev, L. S. Wang, *J. Chem. Phys.* **2011**, *134*, 224304.
- [29] W. Huang, A. P. Sergeeva, H. J. Zhai, B. B. Averkiev, L. S. Wang, A. I. Boldyrev, *Nat. Chem.* **2010**, *2*, 202-206.
- [30] B. Kiran, S. Bulusu, H. J. Zhai, S. Yoo, X. C. Zeng, L. S. Wang, *Proc. Natl. Acad. Sci. U.S.A.* **2005**, *102*, 961-964.
- [31] Z. A. Piazza, W. L. Li, C. Romanescu, A. P. Sergeeva, L. S. Wang, A. I. Boldyrev, *J. Chem. Phys.* **2012**, *136*, 104310.
- [32] A. P. Sergeeva, Z. A. Piazza, C. Romanescu, W. L. Li, A. I. Boldyrev, L. S. Wang, *J. Am. Chem. Soc.* **2012**, *134*, 18065-18073.
- [33] I. A. Popov, Z. A. Piazza, W. L. Li, L. S. Wang, A. I. Boldyrev, *J. Chem. Phys.* **2013**, *139*, 144307.
- [34] Z. A. Piazza, I. A. Popov, W. L. Li, R. Pal, X. C. Zeng, A. I. Boldyrev, L. S. Wang, *J. Chem. Phys.* **2014**, *141*, 034303.
- [35] X. M. Luo, T. Jian, L. J. Cheng, W. L. Li, Q. Chen, R. Li, H. J. Zhai, S. D. Li, A. I. Boldyrev, J. Li, L. S. Wang, *Chem. Phys. Lett.* **2017**, *683*, 336-341.
- [36] W. L. Li, R. Pal, Z. A. Piazza, X. C. Zeng, L. S. Wang, *J. Chem. Phys.* **2015**, *142*, 204305.
- [37] Y. J. Wang, Y. F. Zhao, W. L. Li, T. Jian, Q. Chen, X. R. You, T. Ou, X. Y. Zhao, H. J. Zhai, S. D. Li, J. Li, L. S. Wang, *J. Chem. Phys.* **2016**, *144*, 064307.
- [38] H. R. Li, T. Jian, W. L. Li, C. Q. Miao, Y. J. Wang, Q. Chen, X. M. Luo, K. Wang, H. J. Zhai, S. D. Li, L. S. Wang, *Phys. Chem. Chem. Phys.* **2016**, *18*, 29147-29155.
- [39] W. L. Li, Y. F. Zhao, H. S. Hu, J. Li, L. S. Wang, *Angew. Chem. Int. Ed.* **2014**, *53*, 5540-5545; *Angew. Chem.* **2014**, *126*, 5646-5651.
- [40] W. L. Li, Q. Chen, W. J. Tian, H. Bai, Y. F. Zhao, H. S. Hu, J. Li, H. J. Zhai, S. D. Li, L. S. Wang, *J. Am. Chem. Soc.* **2014**, *136*, 12257-12260.
- [41] Z. A. Piazza, H. S. Hu, W. L. Li, Y. F. Zhao, J. Li, L. S. Wang, *Nat. Commun.* **2014**, *5*, 3113.
- [42] Q. Chen, W. J. Tian, L. Y. Feng, H. G. Lu, Y. W. Mu, H. J. Zhai, S. D. Li, L. S. Wang, *Nanoscale* **2017**, *9*, 4550-4557.
- [43] C. Romanescu, D. J. Harding, A. Felicic, L. S. Wang, *J. Chem. Phys.* **2012**, *137*, 014317.
- [44] D. Y. Zubarev, A. I. Boldyrev, *J. Comput. Chem.* **2007**, *28*, 251-268.
- [45] J. O. C. Jimenez-Halla, R. Islas, T. Heine, G. Merino, *Angew. Chem. Int. Ed.* **2010**, *49*, 5668-5671; *Angew. Chem.* **2010**, *122*, 5803-5806.
- [46] G. Martinez-Guajardo, A. P. Sergeeva, A. I. Boldyrev, T. Heine, J. M. Ugalde, G. Merino, *Chem. Commun.* **2011**, *47*, 6242-6244.
- [47] J. Zhang, A. P. Sergeeva, M. Sparta, A. N. Alexandrova, *Angew. Chem. Int. Ed.* **2012**, *51*, 8512-8515; *Angew. Chem.* **2012**, *124*, 8640-8643.

- [48] D. Moreno, S. Pan, L. L. Zeonjuk, R. Islas, E. Osorio, G. Martinez-Guajardo, P. K. Chattaraj, T. Heine, G. Merino, *Chem. Commun.* **2014**, 50, 8140-8143.
- [49] Y. J. Wang, X. Y. Zhao, Q. Chen, H. J. Zhai, S. D. Li, *Nanoscale* **2015**, 7, 16054-16060.
- [50] Y. J. Wang, X. R. You, Q. Chen, L. Y. Feng, K. Wang, T. Ou, X. Y. Zhao, H. J. Zhai, S. D. Li, *Phys. Chem. Chem. Phys.* **2016**, 18, 15774-15782.
- [51] M. R. Fagiani, X. Song, P. Petkov, S. Debnath, S. Gewinner, W. Schollkopf, T. Heine, A. Felicke, K. R. Asmis, *Angew. Chem. Int. Ed.* **2017**, 56, 501-504; *Angew. Chem.* **2017**, 129, 515-519.
- [52] H. J. Zhai, Y. F. Zhao, W. L. Li, Q. Chen, H. Bai, H. S. Hu, Z. A. Piazza, W. J. Tian, H. G. Lu, Y. B. Wu, Y. W. Mu, G. F. Wei, Z. P. Liu, J. Li, S. D. Li, L. S. Wang, *Nat. Chem.* **2014**, 6, 727-731.
- [53] Q. Chen, W. L. Li, Y. F. Zhao, S. Y. Zhang, H. S. Hu, H. Bai, H. R. Li, W. J. Tian, H. G. Lu, H. J. Zhai, S. D. Li, J. Li, L. S. Wang, *ACS Nano* **2015**, 9, 754-760.
- [54] L. S. Wang, H. S. Cheng, J. Fan, *J. Chem. Phys.* **1995**, 102, 9480-9493.
- [55] X. Chen, Y. F. Zhao, L. S. Wang, J. Li, *Comput. Theor. Chem.* **2017**, 1107, 57-65.
- [56] Y. F. Zhao, X. Chen, J. Li, *Nano Res.* **2017**, DOI: 10.1007/s12274-017-1553-z.
- [57] J. P. Perdew, K. Burke, M. Ernzerhof, *Phys. Rev. Lett.* **1996**, 77, 3865-3868.
- [58] J. P. Perdew, K. Burke, M. Ernzerhof, *Phys. Rev. Lett.* **1997**, 78, 1396-1396.
- [59] C. Adamo, V. Barone, *J. Chem. Phys.* **1999**, 110, 6158-6170.
- [60] R. Bauernschmitt, R. Ahlrichs, *Chem. Phys. Lett.* **1996**, 256, 454-464.
- [61] D. Y. Zubarev, A. I. Boldyrev, *Phys. Chem. Chem. Phys.* **2008**, 10, 5207-5217.
- [62] L. Liu, E. Osorio, T. Heine, *Chem. Asian J.* **2016**, 11, 3220-3224.
- [63] X. Wu, J. Dai, Y. Zhao, Z. Zhuo, J. Yang, X. C. Zeng, *ACS Nano* **2012**, 6, 7443-7453.
- [64] M. J. Frisch, G. W. Trucks, H. B. Schlegel, G. E. Scuseria, M. A. Robb, J. R. Cheeseman, G. Scalmani, V. Barone, B. Mennucci, G. A. Petersson, *et al.*, Gaussian 09 Revision, B.01; Gaussian Inc., Wallingford, CT, **2010**.
- [65] U. Varetto, Molekel 5.4.0.8, Swiss National Supercomputing Center, Manno, Switzerland. **2009**.

B_{33} and B_{34} : Aromatic planar boron clusters with a hexagonal vacancy



Planar Boron Clusters

Q. Chen, W. L. Li, X. Y. Zhao, H. R. Li, L. Y. Feng, H. J. Zhai,* S. D. Li,* L. S. Wang*

Page No. – Page No.

A joint photoelectron spectroscopy and theoretical study is used to probe the structures and chemical bonding of the B_{33} and B_{34} clusters. Both clusters are found to be planar with a hexagonal vacancy, providing key links in understanding the structural evolution of boron clusters. Chemical bonding analyses show that both clusters are aromatic with d bonding similar to polyaromatic hydrocarbons.